Pop5 Protein Tethered Structural Probes of Archaeal RNase P

Undergraduate Research Thesis

Presented in partial fulfillment of the requirements for graduation *with research distinction* in Biochemistry in the undergraduate colleges of The Ohio State University

by

Jamie Nickels

The Ohio State University
2013

Project Advisor: Dr. Mark Foster, Department of Chemistry and Biochemistry

TABLE OF CONTENTS

ABSTRACT

Ribonuclease P (RNase P) is an essential and ubiquitous ribonucleoprotein (RNP) complex that catalyzes the removal of the 5' leader sequence of precursor tRNA molecules. It contains one catalytic RNA subunit in most organisms and a varying number of protein subunits: bacteria ≥1, archaea ≥5, and eukarya ≥10. Due to the complexity of eukaryal RNase P, the RNP complex has only been partially characterized in *Saccharomyces cerevisiae* and *Homo sapiens.* However, because the archaeal ribonuclease P proteins (RPPs) share homology with five of the eukaryal RPPs, archaea such as *Pyrococcus furiosus* (*Pfu*) have been used as model organisms to study the structure and function of the RNP complex. *Pfu* RNase P contains 5 protein subunits: Pop5, RPP30, RPP21, RPP29, and L7Ae. Pop5 and RPP30, as well as RPP21 and RPP29, form heterodimers in the absence of RNA and appear to contribute to catalysis and substrate specificity, respectively.

Structural studies of RNase P have shown that the bacterial protein subunit C5 interacts with the 5' leader sequence of precursor tRNA. Because the archaeal protein subunit Pop5 shares structural homology with C5, it has been hypothesized that Pop5 similarly interacts with the substrate in the archaeal RNase P context. Previously generated Pop5 single cysteine mutants were used to recombinantly express mutant proteins, subsequently purified from *E. coli*, and assayed for function. Next, they were modified with disulfide-linked EDTA-Fe, which upon addition of hydrogen peroxide generates hydroxyl radicals. Hydroxyl radicals are short lived and react with any RNA within ~14 Å. Therefore, RNA molecules within the vicinity of the EDTA-tagged Pop5 subunit will be cleaved, identifying a close RNA-protein contact. By this method, sites of RNA cleavage are detected by primer extension assays using reverse transcriptase and sequence-specific primers, and the resultant DNA fragments resolved on a polyacrylamide gel.

The observed cleavage patterns will provide intermolecular distance restraints allowing Pop5 to be positioned within the holoenzyme complex.

INTRODUCTION

RNase P Background

Sidney Altman won the Nobel Prize in 1985 for his work with RNase P, proving that the RNA subunit of this ribonucleoprotein functions as a catalyst [Altman, 1992; Altman, 2006]. As a true RNA catalyst, RNase P is capable of performing its enzymatic reaction, trans cleavage of the 5' leader sequence of pre-tRNA, without altering the catalyst [Altman, 1999; Guerrier-Takada, 1983]. This finding was remarkable in that biological catalysis is most commonly performed by protein enzymes. Altman's discovery had great impact in part because it provided evidence in favor of the RNA World Hypothesis, which posits that RNA evolutionarily preceded proteins, performing the essential functions of life until the evolution of protein molecules [Poole, 1998].

RNase P catalyzes the removal of the 5' leader sequence of all pre-tRNAs (Figure 1.1). The reaction is thought to involve an S_N2 mechanism by which a Mg^{2+}-hydroxide complex attacks the scissile phosphodiester bond of pre-tRNA causing cleavage between the -1 and +1 positions [Guerrier-Takada, 1986; Cassano, 2004]. This reaction is conserved throughout all domains of life. Up until 2008 this reaction was thought as impossible to perform without the RPR (RNase P RNA), but work with human mitochondrial RNase P showed that some protein-only enzymes could perform the reaction [Holzmann, 2008]. While every other version of RNase P studied contains one catalytic RPR, the number of associated protein subunits or RPPs (RNase P Protein) varies throughout the domains of life. The bacterial enzyme has been found to contain one RPP, archaeal RNase P at least five, and the eukaryal enzyme at least ten [Ellis,

2009; Cho, 2010]. The RPRs alone are catalytically active *in vitro*, but their RPPs are necessary for activity *in vivo* [Altman, 2006].

While the RNase P holoenzyme contains one RPR throughout the three domains of life, the structure and sequences of the RPRs vary substantially (Figure 1.2), with the exception of a core sequence of universally conserved nucleotides [Ellis, 2009; Li, 2004 A]. The RPR is largest in bacteria, while the archaeal and eukaryal RPRs are up to 10-20% smaller [Altman, 2006]. Although the RPRs present in all domains of life have been shown to be catalytically active *in vitro* in high salt buffers [Guerrier-Takada, 1983; Pannucci, 1999; Kikovska, 2007], there are dramatic differences in their activity, with the bacterial RPR as the most active form, followed by archaea and then eukarya [Ellis, 2009]. The differences in *in vitro* activity can be attributed to the structural differences between the RPR sequences. The bacterial RPR contains several structures that resemble key features of protein catalysts, such as the presence of pre-organized substrate binding sites and primary and secondary structure versatility that generates a three-dimensional fold for performing catalysis [Altman, 2006]. The archaeal and eukaryal RPRs on the other hand lack some of these key features thought important for tertiary contacts or for direct interactions with the substrate [Li, 2004 October; Harris, 2001].

Although RNase P primarily catalyzes cleavage of the 5' leader sequence of pre-tRNA, it has also been found to act on other substrates. These include other pre-tRNA like substrates such as pre-10Sa RNA (tmRNA), an intergenic segment of RNA found in the lac operon of *E. coli*, and the riboswitch of the B_{12} coenzyme [Komine, 1994; Li, 2004 May; Altman 2005]. Although RNase P is capable of catalyzing these other reactions, its only universally known reaction is removal of the 5' leader sequence.

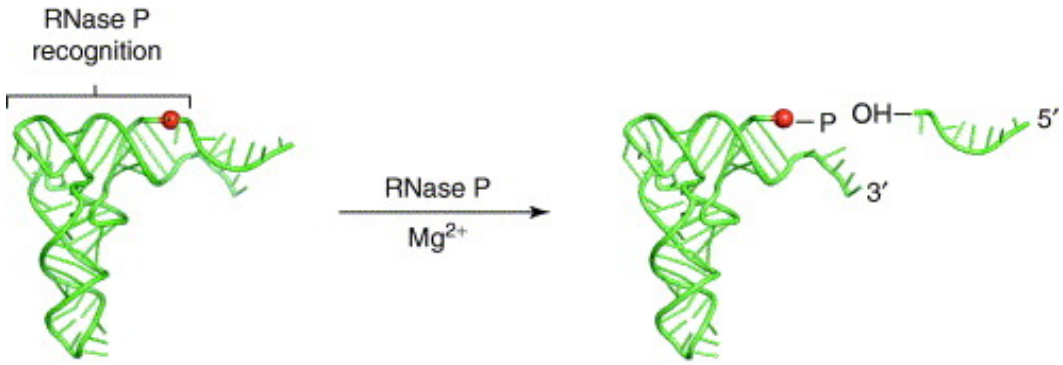

Figure 1.1: RNase P catalyzed cleavage of the pre-tRNA 5' leader sequence. Figure from [Evans, 2006].

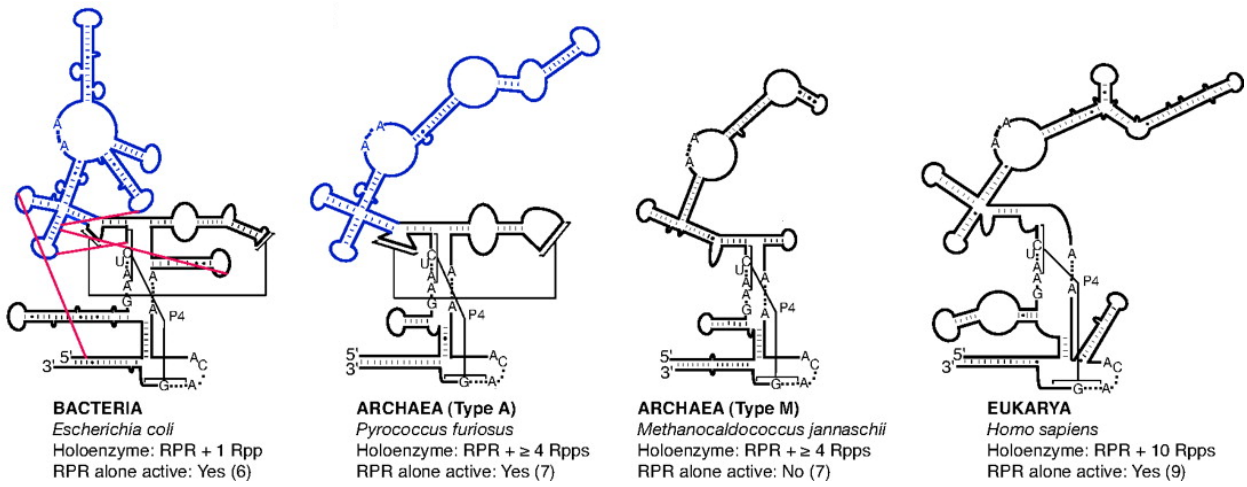

Figure 1.2: Different RNase P RPRs. The S-domains of bacteria and type A archaea are shown in blue. In general, bacterial RPRs are the largest followed by archaea and eukaryotes. As evident from looking at these RPR secondary structures they contain substantial differences in secondary structure as well as size. Figure adapted from [Gopalan, 2007].

Pyrococcus furiosus (Pfu) RNase P

The RNase P holoenzyme has been characterized in several bacteria as well as *Homo sapiens.* However the complexity of eukaryal RNase P can make it difficult to work with. *Pyrococcus furiosus (Pfu),* a hyperthermophilic archaeon, has been chosen as a model organism

because not only is it easier to work with than the eukaryal enzymes, but unlike bacteria all of the archaeal RNase P RPPs have eukaryal homologs [Hall, 2002].

Known archaeal RNase P enzymes possess one catalytic RPR and at least five RPPs. While there is only one RPR present in each archaeal RNase P holoenzyme, their secondary structures fall into two distinct groups, either type A or type M (Figure 1.3)[Ellis, 2009]. *Pfu* RNase P contains the type A RPR, which resembles the bacterial RPR in many of its secondary structural elements, with the exception of the P18 and P13/14 regions present in bacteria, which type A RPRs lack [Ellis, 2009]. On the other hand, the type M RPR more closely resembles the eukaryal version in secondary structure and is only able to process pre-tRNA when the substrate is provided in *cis* [Chen, 2010]. However, all RPRs contain a catalytic or C-domain and a specificity or S-domain. The C-domain is responsible for cleaving the 5' leader sequence of the pre-tRNA, while the S-domain facilitates substrate binding and houses conserved nucleotides that recognize the T-stem loop of the pre-tRNA substrate [Harris, 2003].

The protein subunits present in archaea include Pop5, RPP21, RPP29, RPP30, and the more recently discovered L7Ae (Figure 1.3) [Cho, 2010]. Pop5 and RPP30 form a heterotetramer, while RPP21 and RPP29 form a heterodimer (Figure 1.3) [Crowe, 2011; Amero, 2008]. As mentioned above, the RPPs enhance catalytic activity of the RPRs. The RPP21-RPP29 complex binds to the S-domain of the RPR, enhancing the affinity of the RPR for pre-tRNA [Tsai, 2006; Chen 2010]. The Pop5-RPP30 complex on the other hand binds to the C-domain of the RPR enhancing the rate of cleavage by nearly 100-fold [Tsai, 2006; Chen 2010]. All of the known archaeal RPPs have been shown to share homology with several of the eukaryal proteins. Pop5, RPP21, RPP29, and RPP30 share homology with eukaryal protein subunits of the same name, while L7Ae shares homology with RPP38 [Hall, 2002].

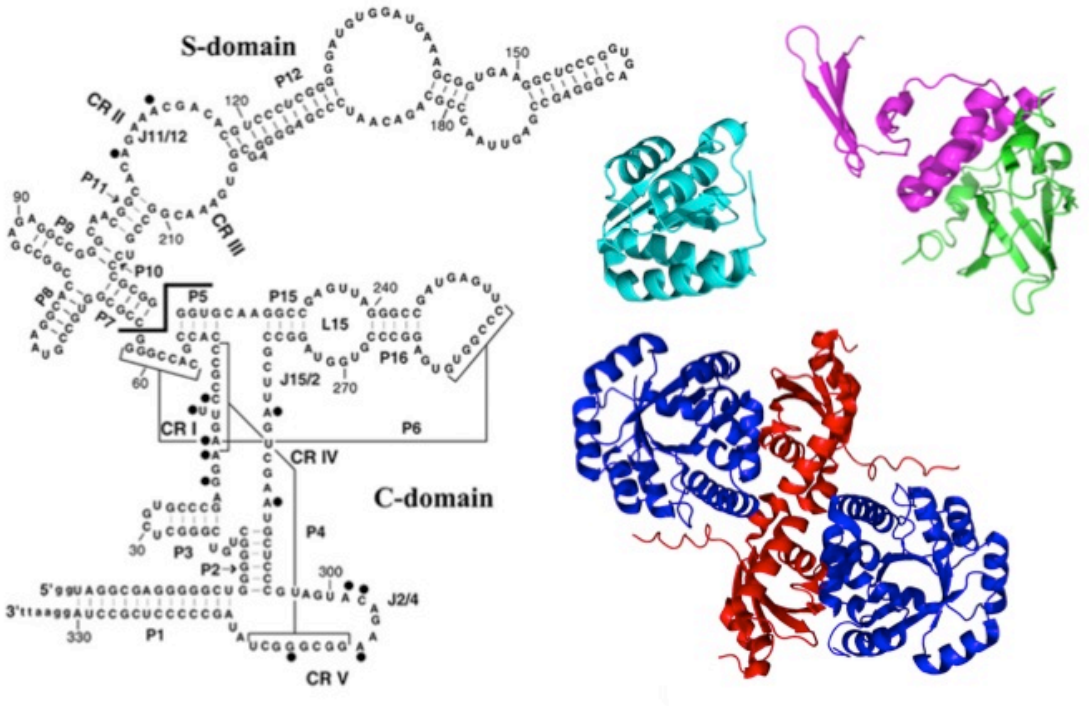

Figure 1.3: Left) *Pfu* RNase P RPR. Figure adapted from [Tsai, 2006]. (Right) *Pfu* RNase P RPPs (RPP30, Pop5, RPP21, RPP29, L7Ae). Pop5 and RPP30 form a heterotetramer, while RPP21 and RPP29 form a dimer. Figures generated from PDB coordinates (Pop5+RPP30 PDB ID: 2CZV, RPP21+RPP29: 2KI7, L7Ae: 2HVY- chain D).

Pop5 Protein Subunit

The Pop5 protein subunit of *Pfu* consists of 120 amino acid residues and weighs 13.7 kDa. *Pfu* Pop5 like the bacterial protein subunit C5, has been shown to interact with the C-domain of the RPR [Tsai, 2006; Reiter, 2010]. Despite this similarity they contain significant differences in primary sequence and secondary structural topology [Wilson, 2006]. However, structural studies using NMR and X-ray crystallography have revealed remarkable 3-dimensional similarities between C5 and Pop5 making them homologous (Figure 1.4a). A major likeness between the two is their similarity to a conserved RNA recognition motif (RRM) domain

[Wilson, 2006]. Differences in primary and secondary structure and similarities in tertiary structure suggests different evolutionary origins [Wilson, 2006].

The bacterial C5 protein has been shown to interact with the distal portion of the 5' leader sequence of pre-tRNA in a cleft near one region of conserved bacterial residues while lacking any interaction with the mature tRNA (Figure 1.4b) [Reiter, 2010; Tsai, 2003]. Due to the homology between C5 and Pop5, Pop5 has been hypothesized to interact with the 5' leader sequence of pre-tRNA as well. This hypothesis has not been rigorously tested.

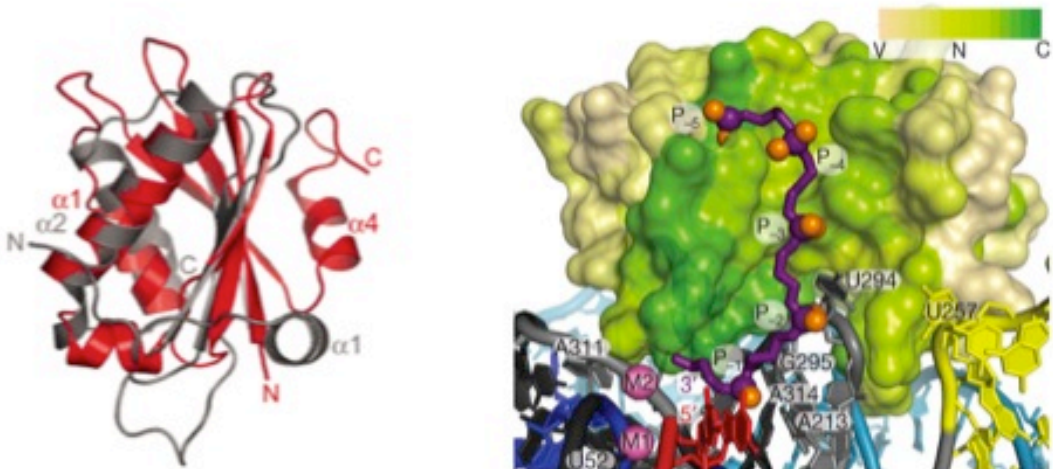

Figure 1.4: Left) Superimposition of Pop5 (red) and C5 (gray) by aligning the a_1 helix of C5 and the a_2 helix of Pop5 reveals structural similarity. From [Wilson, 2006]. (Right) The X-ray crystal structure of *T. maritima* shows C5 (Surface representation of the protein colored by sequence conservation: variable (V), tan; neutral (N), light green; conserved (C), green) to interact with pre-tRNA (purple). From [Reiter, 2010]

OBJECTIVES

Grow and purify the Pop5 single cysteine mutant proteins by transforming *E. coli* BL21 (DE3) cells with previously generated mutant Pop5 plasmids (Dileep Pulukkunat, Gopalan Lab). Perform activity assays on the mutants to determine if they had any deleterious affects on binding specificity or protein folding (in collaboration with Stella

Lai). Modify the mutants at the single cysteine residue with an EPD-Fe moiety that will later be used in a footprinting reaction. Quantify the extent of modification using MALDI mass spectrometry. Perform the EPD-Fe footprinting reaction, use the resultant RPR/pre-tRNA fragments, reverse transcriptase, and sequence specific primers to generate cDNA (performed by Stella Lai). Run the cDNA on an agarose gel to determine the sites of hydroxyl radical mediated cleavage on the RPR/pre-tRNA (performed by Stella Lai). The cleavage sites can then be used to more accurately position Pop5 within the holoenzyme as well as position it with respect to the pre-tRNA substrate.

APPROACH

Protein Tethered Structural Probes

Several methods have been developed to physically map RNA-protein interactions; one of these methods uses an EPD-Fe probe to generate reactive oxygen species that will cleave nearby nucleic acids. Single cysteine mutants of the desired protein must first be generated because EPD-Fe attachment is achieved through the cysteine's thiol group (Figure 2.1) [Hall, 1999]. To avoid coupling probes to native cysteine residues, these must first be mutated out and the cysteine used for attachment must be strategically engineered in at a location on the surface of the protein thought to be near the site of interaction with the target nucleic acid. Ascorbate and hydrogen peroxide is then be added to the modified protein to initiate the reaction. The ascorbate reduces the coordinated Fe(III) to Fe(II), which then reacts with hydrogen peroxide, via the Fenton reaction to generate reactive oxygen species [Hall, 1999]. These reactive oxygen species, in this case a hydroxyl radical, will then attack the ribose sugar of the nucleic acids [Hall, 1999]. Because reactive oxygen species are so short lived within aqueous solutions, they

will only cleave any nucleic acids within 10 Å [Figure 2.2]. Taking into account the 14 Å tether length of the EPD-Fe along with the reactive center gives the probe an effective reach of 22 Å [Hall, 1999].

There are two principal methods used to determine where the hydroxyl radical mediated cleavage of the RNA occurred. The first is direct readout, in which the RNA of interest is labeled with a radioactive tracer at one end, allowing the resultant fragments generated from footprinting to be directly applied to a PAGE gel for analysis. The other method, primer extension, does not require labeled RNA in the footprinting reaction. The resultant fragments then are treated with reverse transcriptase in the presence of labeled sequence-specific DNA primers in order to generate corresponding cDNA which can then be resolved on a PAGE gel for analysis [Figure 2.2].

When footprinting the Pop5 single cysteine mutants with the RPR, primer extension is used due to the large size of the RPR, which due to the limited resolving power of PAGE, would make full sequence coverage of the over 300 nucleotide long RPR difficult using direct readout.

Several factors must be considered when using the protein-tethered footprinting method. First, the effective reach of the probe, which is why the placement of the single cysteine mutants must be done strategically. The flexibility of the probe may also cause variability in the exact residues cleaved from experiment to experiment, but the footprints should remain in the same general area. The reaction yield, which is a low 5-15% can make the footprints hard to distinguish from background noise [Hall, 1999]. This low yield is caused by the short lifetime of the hydroxyl radicals as well as the fact that the dominant chemistry is unproductive reactions of the reagent [Hall, 1999]. It is also important to note that functional assays are a necessary control to ensure that the cysteine mutations do not affect binding specificity or protein folding.

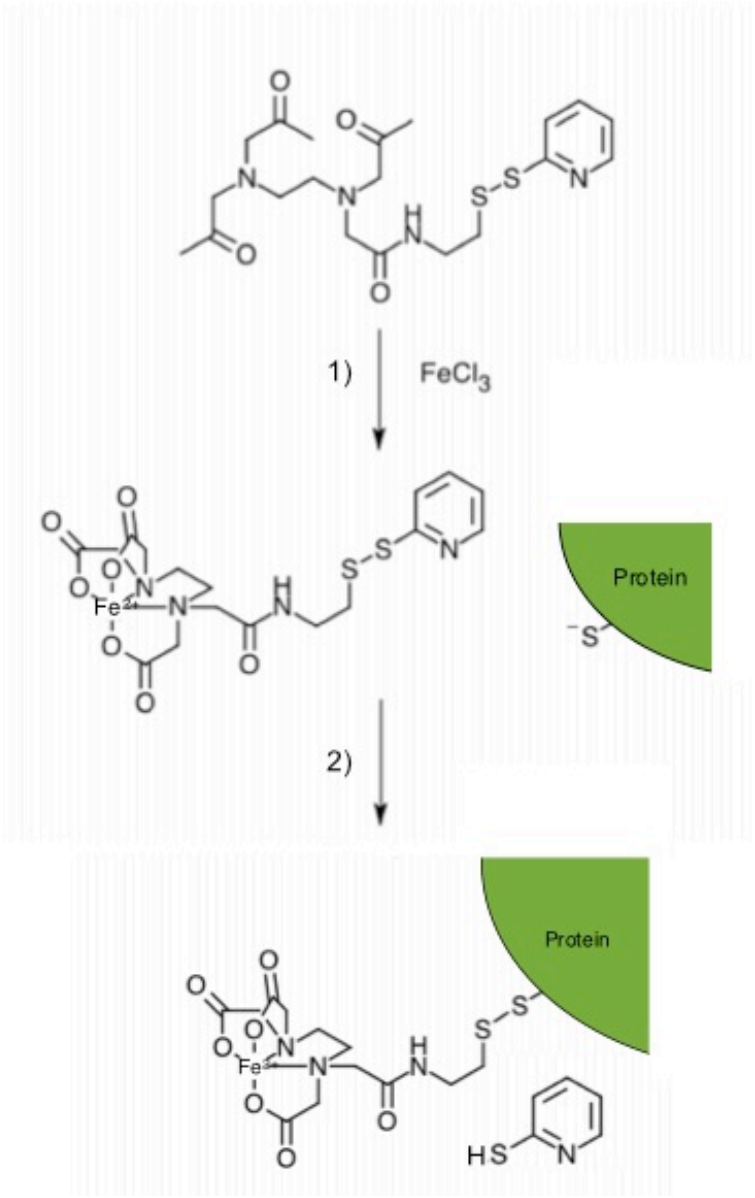

Figure 2.1: Generation of modified mutant proteins. 1) EPD is first reacted with $FeCl_3$ for 15 min. by mixing. 2) The EPD-Fe is then added to the solution of reduced mutant protein forming a disulfide bond by mixing for 30 min. The end product is a modified mutant protein and 2-pyridythiol. The 2-pyridythiol and excess EPD-Fe are removed from the solution using a PD SpinTrap column.

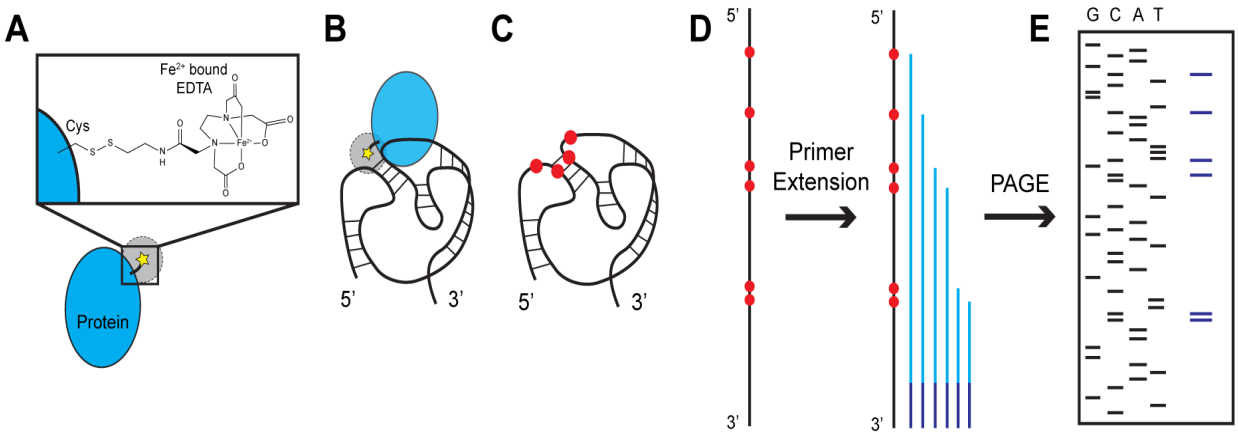

Figure 2.2: A) Modified single cysteine mutant. (B) Addition of ascorbate and H_2O_2 generates short lived hydroxyl radicals via the Fenton reaction which will cleave any RNA within 10 Å of the reactive Fe center. (C) Sites of EPD-Fe mediated cleavage. (D) Treating resultant RNA fragments with reverse transcriptase and sequence specific primers generates cDNA. (E) The corresponding cDNA fragments are then run on a PAGE gel next to a sequencing ladder in order to determine cleavage sites. Figure courtesy of Brandon Crowe.

Selection of Single Cysteine Mutation Sites

Previous structural studies utilizing EPD-Fe probes and other cross-linking methods have been performed on RNase P from several different bacteria mapping the C5 subunit onto the RPR and revealing how C5 interacts with pre-tRNA [Tsai, 2003]. Similar studies have not been performed on archaeal RNase P using C5's homolog Pop5. Strategically selecting residues within the structurally similar region of Pop5 for single cysteine mutations and using EPD-Fe modifications to probe both the pre-tRNA and RPR should elucidate interactions between the selected regions of Pop5 and either RNA. Five residues along the proposed pre-tRNA-Pop5 interface were chosen and introduced by Dileep Pulukkunat (Gopalan Lab) for the single cysteine mutations: A20, K35, I59, I69, and L100 (Figure 2.2). In order to make these single cysteine mutants, Pop5's two native cysteines at positions 42 and 72 were mutated to serines. Previous studies of the C42S, C72S Pop5 mutant found it to have improved solubility over wild type Pop5 with no detrimental effects on structure [Wilson, 2006].

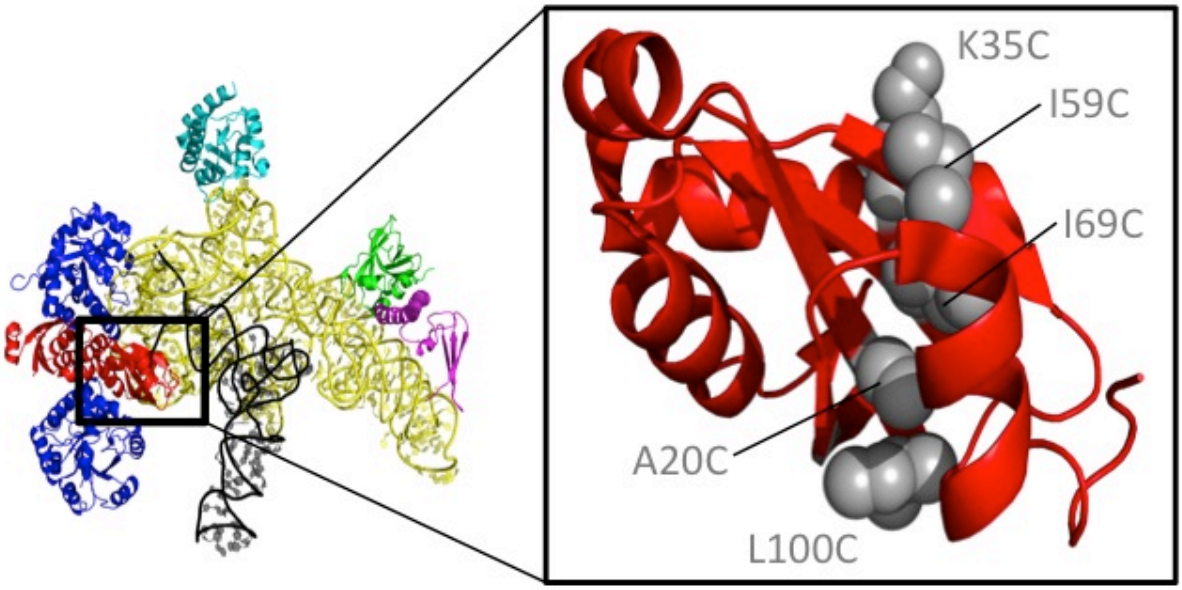

Figure 2.2: Pop5 is hypothesized to interact with the 5' leader sequence of pre-tRNA (shown in black). The residues chosen for the single cysteine mutations are shown in grey and occur along the proposed interface between the two. [Figure courtesy of Brandon Crowe]

MATERIALS AND METHODS

Generation of Single Cysteine Mutant Plasmids

Mutant plasmids were created via QuikChange mutagenesis using the pET-33b plasmid vector with the Pop5 gene cloned in via the 3' *Eco*RI site and sequence-specific primers containing the desired mutations. The Pop5 gene was expressed under the T7 promoter with the plasmid being resistant to the antibiotic kanamycin. Mutagenesis was verified using DNA sequencing immediately following creation of the plasmids as well as before expression of the Pop5 mutant proteins for use in the footprinting experiments [Dileep Pulukkanat, unpublished].

Expression of Pop5

Pop5 single cysteine mutant plasmids were transformed into Rosetta BL21 (DE3) cells using electroporation. Rosetta BL21 (DE3) cells are resistant to chloramphenicol and facilitate

expression of genes that encode rare *E. coli* codons. After letting the cells recover in Luria broth (LB) for 30 min. at 37 °C they were plated onto LB agar plates containing kanamycin (30 μg/mL) and chloramphenicol (34 μg/mL). Following overnight growth at 37 °C, one colony was placed into a 100 mL starter culture of LB containing kanamycin (30 μg/mL) and chloramphenicol (34 μg/mL) and grown for ~12 hours at 37 °C with 250 RPM agitation. A 1 L culture was then created by adding 10 mL of the starter culture to 1 L of LB with kanamycin (30 μg/mL) and chloramphenicol (34 μg/mL). The 1 L culture was then grown at 37 °C and 250 RPM agitation until OD_{600} reached 0.6 – 0.8. Once the appropriate OD was attained the culture was induced to grow the mutant proteins using IPTG (0.5 mM). After 4 hours of induction at 37 °C and 250 RPM agitation, the cells were harvested by centrifugation at 5,000 RPM for 20 min. at 4 °C. The resultant cell pellet was then transferred to a 50 mL Falcon tube and stored at -20 °C until purification.

Pop5 Mutant Protein Purification

The Pop5 mutant protein pellet was resuspended in 30 mL of lysis buffer (25 mM Tris pH 7.3, 25 mM KCl, 50 mM DTT) and lysed using sonication on ice (50 amplitude, 5 second pulses; 5' on, 3 off, 5' on, etc.). The lysate was then centrifuged at 15,000 RPM for 30 min. Next, the soluble portion of the lysate was decanted and heated to 75 °C for ~20 min. in order to precipitate the non-heat stable *E. coli* proteins. Meanwhile, the insoluble portion of the lysate was resuspended in resuspension buffer (8 M urea, 50 mM Tris pH 7.3, 250 mM KCl, 50 mM DTT) and sonicated. The heated supernatant and sonicated pellet were centrifuged at 15,000 RPM for 15 min. Because Pop5 is present in both the heat soluble and soluble portion of the resuspended cell lysate, the supernatant from the heated and sonicated solutions was combined and filtered using a 0.45 μM filter. After cleaning a 5 mL SP FF cation exchange

column with 5 column volumes of water, 6 M guanidium-HCl, water, and then equilibrating using resuspension buffer, the combined supernatant solution was then loaded onto the column. After washing the column with 10 mL of resuspension buffer to remove any unbound contaminants the column was incubated at 75 °C for ~20 min. to refold the protein. Following refolding the column was placed onto the FPLC and the protein was eluted by running a salt gradient from 25 mM to 2 M KCl. In general the Pop5 mutants were eluted between 1.2-1.6 M KCl. Based on the FPLC chromatogram, fractions suspected to contain protein were run on an SDS-PAGE gel. Once it was determined which fractions contained protein, they were combined and dialyzed into dialysis buffer (10 mM NaAc pH 5, 15 μM NaN_3, thoroughly degassed).

EPD-Fe Modification of Pop5 Single Cysteine Mutants

The EPD-Fe modification protocol was based off a modified version of the procedure established by Hall et al. In which the thiol group of the single cysteine mutants were reduced by addition of 5 mM DTT in preparation for the modification reaction. The samples were then dialyzed into the Pop5 storage buffer (10 mM NaAc, 15 μM NaN_3) to rid them of the DTT. EPD and $FeCl_3$ were calculated to be in 10 fold excess over the single cysteine mutants and were reacted together first in absence of the protein by mixing for ~15 min. After the EPD and Fe had been reacted the single cysteine mutants were added to solution and reacted by mixing for ~30 min. In order to clean up the reaction, ridding the solution of any side products and excess EPD-Fe, a GE PD SpinTrap G-25 column was used. The modified and unmodified proteins were then either dialyzed into 50 mM acetic acid for lyophilization or aliquoted into 5 μL portions for later use in footprinting. After overnight lyophilization the protein samples were resuspended in water and used to quantify the extent of the modification reaction via MALDI mass spectrometry.

EPD-Fe Mediated Footprinting and Activity Assays (performed by Stella Lai)

After generating the EPD-Fe modified mutants for Pop5 the footprinting reactions could be performed. This was done by first reconstituting the RNase P holoenzyme (Pop5+RPP21+RPP29+RPP30+L7Ae+RPR) with Mg^{2+} using the modified or unmodified mutant protein. Hydrogen peroxide and ascorbate were then added to the holoenzyme solution, generating hydroxyl radicals. The resultant RPR/pre-tRNA fragments were then treated with reverse transcriptase and sequence specific primers to generate corresponding cDNA fragments. In order to determine the sites of cleavage the cDNA fragments were then run on a polyacrylamide gel along with a sequencing ladder. The Pop5 mutants will also be footprinted with the pre-tRNA alone and by reconstituting the holoenzyme in complex with pre-$tRNA^{Tyr}$ in the presence of Ca^{2+} in an attempt to slow the rate of substrate cleavage [Kasakov, 1991]. While Ca^{2+} decreases the rate of substrate cleavage, previous studies have shown that replacing Mg^{2+} with Ca^{2+} has no effect on the binding ability of the bacterial RPP and tRNA to the holoenzyme [Talbot, 1994; Smith, 1992]. Using Ca^{2+} also promotes proper folding of the RPR [Harris, 1997], making it an ideal candidate to replace Mg^{2+} in the fooprinting experiments involving the pre-tRNA substrate.

RESULTS

Following the established protocols the Pop5 single cysteine mutants were successfully over-expressed in Rosetta BL21(DE3) cells and purified by chromatographic methods (Figure 3.1). Typical yield from these purifications was 15-25 mg/L culture.

Although the Pop5 mutants were over 90% pure before using the SP column this step was performed for two reasons. First, the presence of any contaminant protein with a cysteine would be modified with the rest of the sample and may interact with either the RPR or pre-tRNA causing false footprints. Second, the loss of Pop5 mutant protein in this step is minimal. After purification all mutants were then modified for use in the footprinting assays. MALDI mass spectrometry was used to assess the extent of modification by determining recording the molecular weight of each mutant before and after modification with EPD-Fe (Figure 3.2, Table 3.1). The masses of the Pop5 modified and unmodified mutants were all within 0.10% of the expected mass. A shoulder or peak corresponding to unmodified protein was present in all the modified sample spectra, but the majority present in solution was modified and therefore sufficient for use in footprinting.

Footprinting of the Pop5 mutants with the RPR using a primer, which annealed to the 3' end of the RPR yielded one clear band from the K35C modified mutant (Figure 3.3). This band corresponds to the P12 region of the S-domain. Due to the limited resolution of the sequencing lanes it was hard to determine exactly which nucleotide this footprint corresponds to.

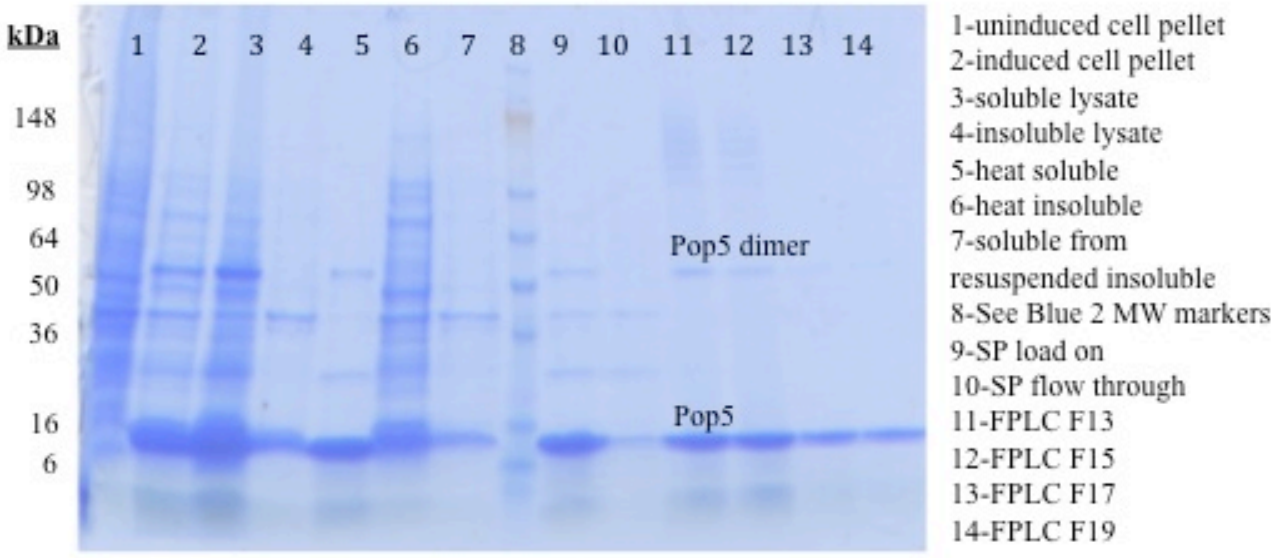

Figure 3.1: Characteristic Pop5 purification (L100C) PAGE gel. As the purification progresses the solution becomes more and more pure until fractions 15 and 16 of the FPLC where only Pop5 is present in solution. Pop5 will readily form dimers in solution.

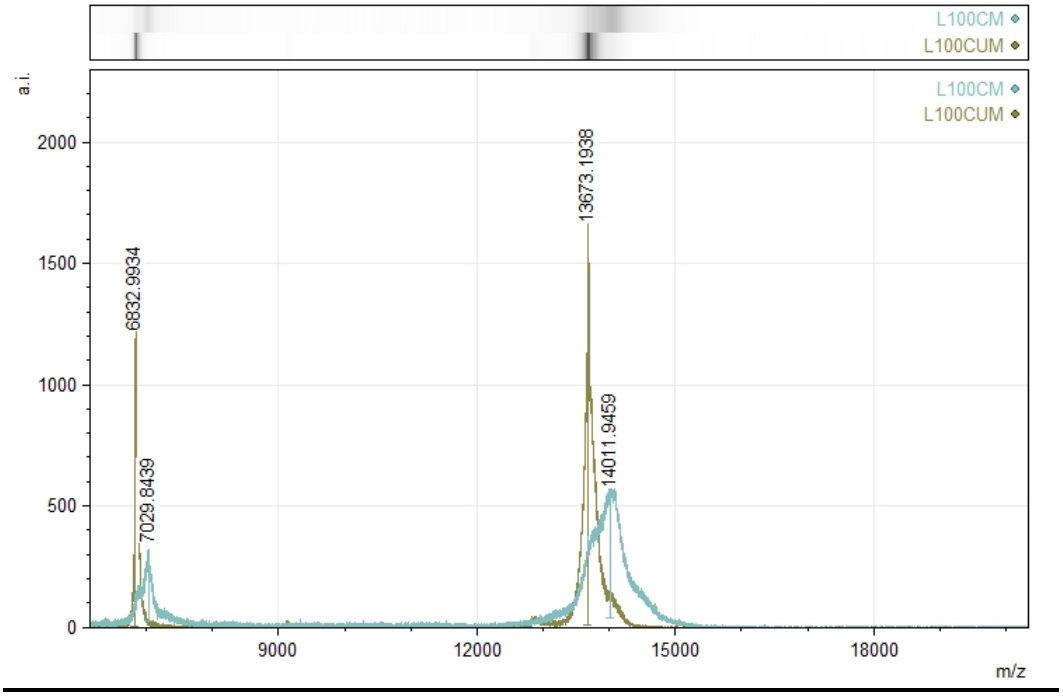

Figure 3.2: MALDI mass spectrum of typical Pop5 modified and unmodified proteins (L100C; modified in blue, unmodified in green). Although the bulk of the protein has been successfully modified, the broadness of the peak indicates the presence of unmodified protein.

Pop5 Mutants	Expected Wt.	MALDI Wt.	Difference
A20C UM	13707.97	13703.33	4.64
A20C M	14109.77	14104.76	5.01
K35C UM	13650.87	13655.76	-4.89
K35C M	14052.67	14041.76	10.91
I59C UM	13665.89	13666.63	-0.74
I59C M	14011.89 (-Fe)	14013.17	-1.28
I69C UM	13665.89	13663.91	1.98
I69C M	14067.69	14067.15	0.54
L100C UM	13665.89	13663.99	1.90
L100C M	14011.89 (-Fe)	14011.95	-0.06

Table 3.1: Comparison of theoretical (calculated using ExPaSY) and experimental weights (calculated using MALDI) of modified and unmodified Pop5 single cysteine mutants. Weights of all Pop5 mutants modified and unmodified were within 10 Da of the expected weight. However, the MALDI mass of some of the mutants suggested the iron was not chelated, it is possible the iron fell off during the actual MALDI process.

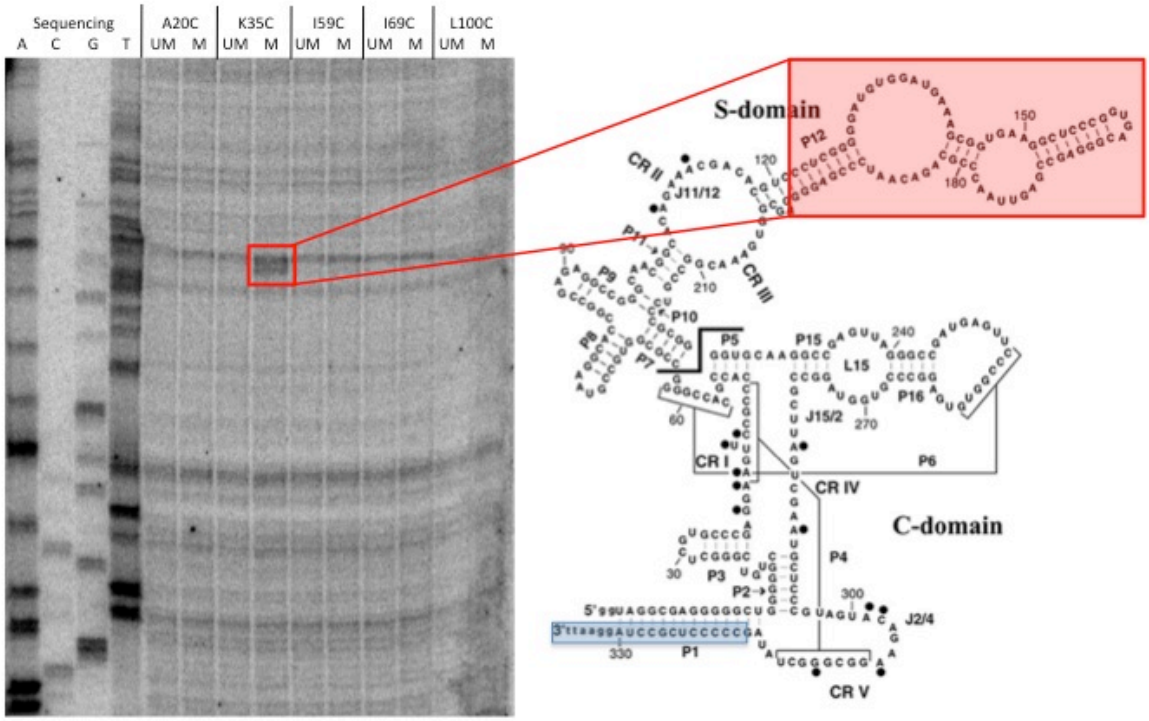

Figure 3.5: Pop5 mutants footprinted with the RPR. The footprint observed for K35C corresponds to the P12 region of the S-domain. Due to the poor quality of the sequencing lanes it is hard to determine which nucleotide the footprint corresponds to exactly. The primer used in this experiment annealed to the 3' end of the RPR (shown in blue).

DISCUSSION

The Pop5 single cysteine mutants were successfully purified following the established protocol. Dimer formation was noted in the Pop5 mutants, which has been observed in wild type Pop5 as well. The pure mutant proteins were then modified with the EPD-Fe probes and the extent of modification was determined using MALDI mass spectrometry. The observed masses of the modified and unmodified Pop5 mutants corresponded well with the expected weights (calculated using ExPASy), falling within 0.10%. Two of the modified Pop5 mutants appeared to be missing the chelated iron. This "falling off" of the iron may be due to the MALDI process, which involves the use of a laser to ionize the sample. The MALDI spectra also revealed that none of the samples had been 100% modified, due to the presence of shoulders and visible peaks corresponding to the unmodified weights of the proteins. However, the majority of all the samples were successfully modified making them suitable for use in the footprinting experiments.

Footprinting of the five Pop5 mutants with the RPR resulted in one clear band from the K35C modified mutant, which corresponds to the P12 region of the S-domain. This result is surprising since it seems to contradict enzymatic data and holoenzyme model which predict the Pop5 subunit binds the C-domain. Previous footprinting studies with RPP29, one of the other RPPs, and the RPR using the EPD-Fe method also produced a footprint in the P12 region. Most of the observed footprints for RPP29's single cysteine mutants R75C and K88C were located within the P9 region of the S-domain. R75C however, produced one footprint within the P12 region as well (Figure 4.1) [Smith, 2011]. This suggests that perhaps P12 plays a role in formation of the holoenzyme. The presence of the P12 footprints may also be due to the excess modified protein used during the footrpinting reaction. This would suggest that P12 may act as a

site for weak secondary binding. Another surprising result of the Pop5-RPR footprinting was that K35C, I59C, and I69C did not footprint to the C-domain. While these mutants were designed specifically to detect interactions between Pop5 and the pre-tRNA, the holoenzyme model still predicts these three residues to be within 10 Å of the RPR. A possible explanation for this lack of interaction is the fact that the Pop5 mutants have only been footprinted in the presence of the RPR. Conformational changes upon addition of the pre-tRNA substrate to the holoenzyme may cause the Pop5 subunit to move closer to the RPR, producing footprints. This is why it is essential that both the pre-tRNA alone and the RPR + pre-tRNA be footprinted with the Pop5 mutants in the future.

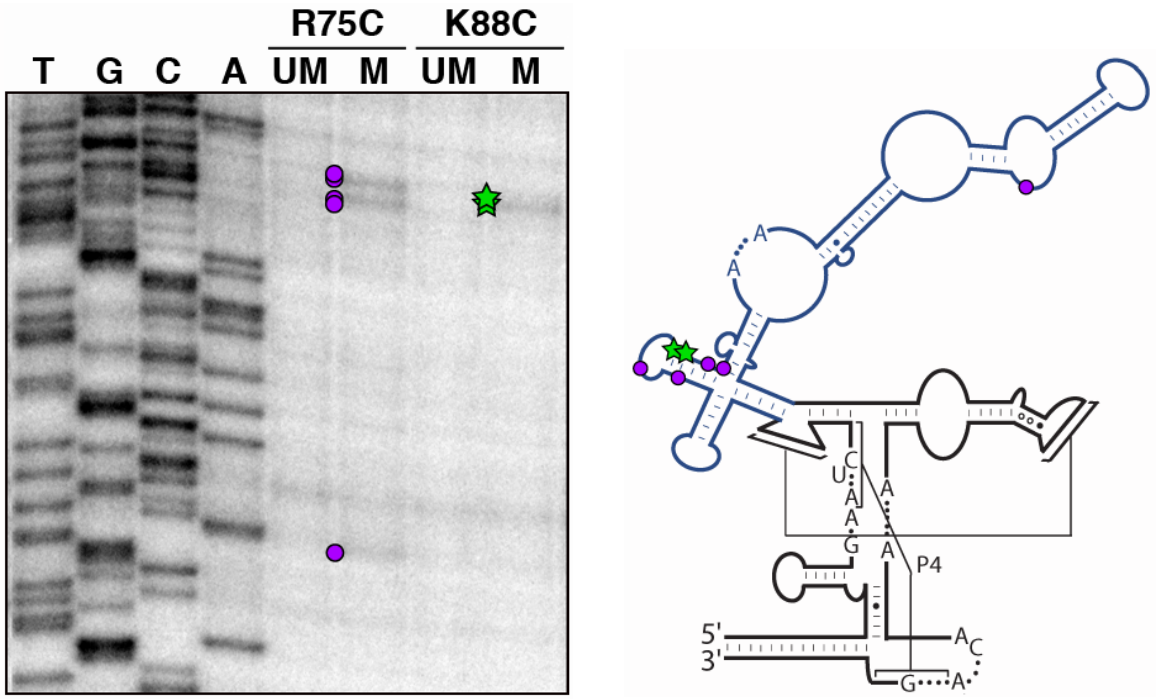

Figure 4.1: Footprinting of the RPP29 mutants R75C and K88C with the RPR. Most of the footprints were located within the P9 region of the S-domain. R75C produced one footprint within the P12 domain similar to K35C.

FUTURE DIRECTIONS

In order to test for reproducibility footprinting of the Pop5 mutants and the RPR must be repeated using the same and different primers. Footprinting experiments should also be performed with the Pop5 mutants using pre-tRNA^{Tyr} as the substrate both in the presence of the RPR and in its absence. To determine if any of the introduced cysteine mutations had deleterious effects on Pop5 folding or formation of the holoenzyme complex activity assays will be performed.

ACKNOWLEDGEMENTS

I would like to thank Stella Lai for performing the footprinting reactions and other general guidance, Brandon Crowe for 3-D models of the RNase P holoenzyme and its protein subunits as well as his Pop5 knowledge, Dileep Pulukkunat for generating the Pop5 mutant plasmids and Yiren Xu for generating the P29 mutant plasmids. I thank Dr. Foster for the privilege to work in his lab as well as the other members of the Foster and Gopalan Labs.

REFERENCES

Altman, S. "Enzymatic Cleavage of RNA by RNA." Nobel Lectures, Chemistry 1981-1990, Ed. Malmström, B.G. (World Scientific Publishing Co., Singapore, 1992).

Altman, S., Gopalan, V., "Ribonuclease P: structure and catalysis." Third Edition ed. The RNA World, ed. R. Gesteland, T. Cech, and J. Atkins. 2006: Cold Spring Harbor Laboratory Press.

Altman, S., Kirsebom, L. "Ribonuclease P." *The RNA World.* (Gesteland, R. F., Cech, T. & Atkins,J. F., eds), pp. 351–380, CSH Laboratory Press, Cold Spring Harbor, NY.

Altman, S., Wesolowski, D., Guerrier-Takada, C., Li, Y. "RNase P cleaves transient structures in some riboswitches." PNAS. 2005 August. 102(32): 11284-11289.

Amero, C., et al. “Solution structure of Pyrococcus furiosus RPP21, a Component of the Archaeal RNase P Holoenzyme, and Interactions with Its RPP29 Protein Partner.” Biochemistry. 2008. 47: 11704-11710.

Boomershine et al. “Structure of Mth11/*Mth* Rpp29, an essential protein subunit of archaeal and eukaryotic RNase P.” PNAS. 2003 December; 100(26): 15398-15403.

Cassano A.G., Anderson V.E., and Harris M.E. “Analysis of solvent nucleophile isotope effects: Evidence for concerted mechanisms and nucleophilic activation by metal coordination in non-enzymatic and ribozyme-catalyzed phosphodiester hydrolysis.” *Biochemistry.* 2004; 43: 10547–10559.

Chen, W., Pulukkanat, D., Cho, I., Tsai, H., Gopalan, V. “Dissecting functional cooperation among protein subunits in archaeal RNase P, a catalytic ribonucleoprotein complex.” Nucleic Acids Res. 2010 December; 38(22): 8316-8327.

Cho, I., Lai, L., Susanti, D., Mukhopadhyay, B., and Gopalan, V., “Ribosomal protein L7Ae is a subunit of archaeal RNase P,” PNAS, vol. 107, no. 33, pp. 14573–14578, 2010.

Crowe, B., et al. “Assembly of the Complex between Archaeal RNase P Proteins RPP30 and Pop5.” Archaea, vol. 2011, Article ID 891531, 12 pages, 2011. doi:10.1155/2011/891531

Ellis, C., Brown, J. “The RNase P family.” RNA Biology. 2009 September/October. 6(4): 362-369.

Evans, D., Marquez, S., Pace, N. “RNase P: interface of the RNA and protein worlds.” Trends in Biochemical Sciences. 2006 June; 31(6): 333-341.

Gopalan, V. “Unifomity amid diversity in Rnase P.” PNAS. 2007 Feb; 104(7): 2031-2032.

Guerrier-Takada, C., Gardiner, K., Marsh, T., Pace, N., Altman, S. “The RNA Moiety of Ribonuclease P Is the Catalytic Subunit of the Enzyme.” Cell. 1983 December; 35: 849-857.

Guerrier-Takada C., Haydock K., Allen L., and Altman S. “Metal ion requirements and other aspects of the reaction catalyzed by M1 RNA, the RNA subunit of ribonuclease P from *Escherichia coli*.” *Biochemistry.* 1986; 25: 1509–1515.

Hall, K., Fox, R. “Directed Cleavage of RNA with Protein-Tethered EDTA-Fe.” Methods. 1999 May. 18(1): 78-84.

Hall, T., Brown, J. “RNase P has multiple protein subunits homologous to eukaryotic RNase P proteins.” RNA. 2002 March; 8(3): 296-306.

Harris, J., Haas, E., Williams, D., Frank, D., Brown, J. “New insight into RNase P RNA structure from compartive analysis of the archaealRNA.” RNA. 2001; 7:220-232.

Harris, M., Christian, E. “Recent insights into the structure and function of the ribonucleoprotein enzyme ribonuclease P.” Curr Opin Struct Biol. 2003 June; 13(3): 325-333.

Harris, M., Kazantsev, A., Chen, J., Pace, N. “Analysis of the tertiary structure of the ribonuclease P ribozyme-substrate complex by site-specific photoaffinity crosslinking.” RNA. 1997 June; 3(6): 561-76.

Holzman, J., et al. “RNase P without RNA: identification and functional reconstitution of the human mitochondrial tRNA processing enzyme.” Cell. 2008. 135: 462-474.

Kasakov, S., Altman, S. “Site-specific cleavage by metal ion cofactors and inhibitors of M1 RNA, the catalytic subunit of RNase P from *Escherichia coli*.” PNAS. 1991 October. 88: 9193-9197.

Kikovska, E., Svard, S.G., Kirsebom, L.A. “Eukaryotic RNase P RNA mediates cleavage in the absence of protein.” PNAS. 2007 Feb; 104(7): 2062-7.

Kim, K., Liu, F. “Inhibition of gene expression in human cells using RNase P-derived ribozymes and externl guide sequences.” Biochim Biophys Acta. 2007 Nov-Dec. 1769(11-12): 603-612.

Komine, Y., Kitabatake, M., Yokogawa, T., Nishikawa, K., Inokuchi, H. “A tRNA- like structure is present in 10Sa RNA, a small stable RNA from Escherichia coli.” PNAS. 1994 September; 91:9223-9227.

Li, Y., Altman, S. “In search of RNase P from microbial genomes.” RNA. 2004 October; 10(10): 1533-1540.

Li, Y., Altman, S. “Polarity Effects in the Lactose Operon of Escherichia coli.” JMB. 2004 May; 339(1): 31-39.

Pannucci, J. et al. “RNase P RNAs from some Archaea are catalytically active.” PNAS. 1999 July; 96(14): 7803-7808.

Poole, A., Jeffares, D., Penny, D. “The Path from the RNA World.” J. Mol. Evol. 1998; 46: 1-17.

Reiter et al. “Structure of a bacterial ribonuclease P holoenzyme in complex with tRNA.” Nature. 2010 December; 468: 784-789.

Sidote, DJ., Hoffman, DW. “Structure of an archaeal homologue of ribonuclease P protein Rpp29.” Biochemistry. 2003 November; 42(46): 13541-50.

Smith, D., Burgin, A., Haas, E., Pace, N. “Influence of metal ions on the ribonuclease P reaction. Distinguishing substrate binding from catalysis.” The Journal of Biological Chemistry. 1992 Feb; 267: 2429-2436.

Smith, I. “Application of Site-directed Metal Chelation Techniques to Structure Determination of Pyrococcus furiosus RNase P.” Undergraduate Research Thesis. Department of Chemistry and Biochemistry, The Ohio State University, Columbus, OH.

Talbot, S.J., Altman, S. “Kinetic and thermodynamic analysis of RNA-protein interactions in the RNase P holoenzyme from Escherichia coli.” Biochemistry. 1994 Feb; 33(6): 1406-11.

Tsai et al. “Molecular Modeling of the Three-dimensional Structure of the Bacterial RNase P Holoenzyme.” JMB. 2003; 325:661-675.

Tsai, H., Pulukkunat, D., Woznick, W., Gopalan, V. “Functional reconstitution and characterization of *Pyrococcus furiosus* RNase P.” PNAS. 2006; 103(44):16147-16152.

Wilson et al. “Structure of Pfu Pop5, an archaeal RNase P protein.” PNAS. 2006 November. 103: 873-878.